New insights on the Dora Maira vs Piedmont Zone boundary (middle Susa Valley, NW Alps): lithostratigraphic setting and tectono-metamorphic evolution

Ivano Gasco[1*], Marco Gattiglio[1] and Alessandro Borghi[2]

[1] Dipartimento di Scienze della Terra, Università di Torino, Via Valperga Caluso 35, I-10125 Torino, Italy

[2] Dipartimento di Scienze Mineralogiche e Petrologiche, Università di Torino, Via Valperga Caluso 35, I-10125 Torino, Italy

* Corresponding Author**:** Phone: +39 011 6705335; Fax: +39 011 6705339; E-mail: ivano.gasco@unito.it

Abstract. A new detailed mapping allowed to better understand the tectonic relationships between the Dora-Maira Massif and the Piedmont Zone in the middle Susa Valley. Four deformation phases were identified: pre-D_1 represents the eclogite facies stage while D_1 developed under greenschist facies conditions, transposed the early foliation and was responsible for the development of the regional schistosity S_1. D_2 is characterized by close to open folds with N dipping axial surfaces and finally, D_3 developed macro-scale folds with E-dipping axial planes. Structural analysis allowed to infer a relative timing for the tectonic contact between the two nappes which were coupled after the eclogite facies metamorphism but before the development of the S_1 foliation under greenschist facies conditions. Petrographic investigation of metapelite samples allowed to identify two main metamorphic assemblages within the Dora-Maira polymetamorphic basement: M1 (Phe + Pg + Cld + Grt + Chl I + Qtz + Rt) defines the pre-S_1 foliation while M2 (Ms + Pg + Ab + Chl II + Qtz + Ilm ± Bt) assemblage is related to the regional foliation S_1. Pseudosection modelling of a garnet-chloritoid micaschist allowed to reconstruct the Alpine PT path of the northern Dora Maira Massif which reached eclogite facies conditions at 18-20 kbar and 515-525 °C (M1/pre-S_1 event) and then was exhumed during increasing T (10-11 kbar and 555-565°C). The M2 assemblage defining the S_1 regional foliation developed at $P < 7$ kbar and $T < 575$ °C. According to the structural evolution the tectonic coupling between Dora-Maira and Piedmont Zone took place during exhumation along the subduction channel.

Keywords: Western Italian Alps, Dora-Maira Massif, lithostratigraphy, structural evolution, pseudosection, PT

path.

Introduction

The understanding of the relative timing of the tectonic coupling between oceanic lithosphere and continental crust is very important to unravel the tectono metamorphic evolution of the Alpine mountain belt. However, this argument is still controversial, indeed Lapen et al. (2007), on the base of geochronological data and PTt path analysis, have proposed that the Monte Rosa-Gran Paradiso Massifs were coupled to the Zermatt-Saas Unit under eclogite-facies conditions and were exhumed together by a buoyancy-driven process. Pleuger et al. (2005) suggested that tectonic coupling of the Monte Rosa Massif and the Zermatt-Saas Unit was achieved before the greenschist facies metamorphic re-equilibration. On the contrary, Kassem & Ring (2004) proposed that the Gran Paradiso has been coupled to the Zermatt-Saas Unit early during subduction under brittle conditions. Recently, Gasco et al. (2009) inferred that the Gran Paradiso and the lower Piedmont Zone were coupled during exhumation after the eclogite facies stage according to the structural relationships between the two nappes. No structural evolution is available for the contact between the northern Dora Maira Massif and the Piedmont Zone despite recent field survey (Carraro et al., 2002; Sacchi et al., 2004).

In this paper we present a detailed study using a multidisciplinary approach based on lithostratigraphy, structural analysis, petrography and petrology that allowed to establish the relative timing for the tectonic coupling between the Northern Dora-Maira and the Piedmont Zone along the Susa Valley. The PT conditions of the tectonic coupling are constrained by the reconstruction of the Dora-Maira PT exhumation path.

Geological setting

The Dora-Maira Massif

The Dora Maira Massif is the southernmost of the three Internal Crystalline Massifs which represent, together with the Monte Rosa and the Gran Paradiso, basement nappes of the inner Penninic Domain in the Western Italian Alps (e.g. Schmid et al., 2004). The Dora Maira Massif (Fig. 1) consists of different tectonic slices of continental basement with different early-Alpine peak-pressure metamorphism. These tectonic slices can be subdivided into three main tectonic units.

The Lower Monometamorphic Unit also known as Sanfront-Pinerolo Unit (Vialon, 1966; Borghi et al., 1984; Henry et al., 1993) is characterized by metasediments and orthogneisses. The detrital sequence consists of meta-conglomerates, meta-arkoses and graphite-bearing meta-pelites, which are intruded by middle-Carboniferous to lower-Permian (306-268 Ma; Bussy and Cadoppi, 1996) magmatic bodies ranging in composition from dioritic to granitic. The Sanfront-Pinerolo represents the lowest tectonic unit exposed in the axial zone of Western Alps and may represent the distal part of the European Briançonnais terrain (Avigad et al., 1993). Blueschist facies assemblages are widespread in the northern part while eclogite facies assemblages were never reported (Borghi et al., 1985; Wheeler, 1991). PT estimations on the Lower Unit are scarce and suggest a re-equilibration stage at 530-550 °C and 6.0-7.5 kbar in the metapelites (Avigad et al., 2003).

The upper Polymetamorphic Unit (Vialon, 1966; Borghi et al., 1984) is made of metapelites and orthogneisses with minor Mesozoic cover. The polymetamorphic metapelites consist of micaschists with rare metabasites and marbles intercalations; pre-Alpine relics attributed to the Variscan metamorphism are represented by garnet-muscovite-sillimanite and pseudomorphs after cordierite, spinel, andalusite and staurolite (Cadoppi, 1990; Compagnoni et al, 1993 with references therein). The orthogneisses consist of polymetamorphic granodiorites (Vialon, 1966) of upper-Ordovician age (455-459 Ma, Bussy and Cadoppi, 1996) preserving red-biotite of Variscan age, and of monometamorphic granites and monzogranites of lower-Permian age (267-279 Ma, Bussy and Cadoppi, 1996). In the northern part of the Massif the Mesozoic cover consists of quartzites, marbles and calcschists (Michard, 1967; Caron, 1977; Pognante, 1980; Marthaler et al., 1986; Tallone, 1988, 1990) while it is represented by micaschists, acidic metavolcanites and metaquartzites (Vialon, 1966; Michard, 1967; Michard et al., 1993) in the southern part. According to some authors (Sandrone et al., 1993 with references therein) the metavolcanites of Vialon (1966) are instead metagranites. The Upper Polymetamorphic unit is metamorphosed under eclogite facies conditions at 10-15 kbar and 450-550 °C (Borghi et al., 1985, Pognante and Sandrone, 1989; Cadoppi, 1990; Chopin et al., 1991, Borghi et al., 1996).

In the southern Dora-Maira between the Lower and the Upper Units a coesite-bearing polymetamorphic unit has been identified (Chopin, 1984; Chopin et al., 1991) consisting of orthogneisses and subordinate metapelites, marbles and metabasites which underwent UHP metamorphism at 35 Ma (Gebauer *et al.*, 1997).

On the contrary, no geochronological data are available for the Upper Polymetamorphic and the Lower Monometamorphic Unit.

The Piedmont Zone

The Piedmont Zone (Fig. 1), representing the remnant of the Tethys Ocean, consists of two main units, the lower and the upper one, respectively known as the Zermatt-Saas Unit (ZS) and the Combin Unit (CO) in the southern Valais and northern Aosta Valley (Bearth, 1967; Dal Piaz, 1974; Dal Piaz and Ernst, 1978; Dal Piaz, 1999). South of the Aosta Valley and in the Piedmont-French Alps the Piedmont Zone is classically known as Schistes Lustrés (for a review see: Lemoine and Tricart, 1986; Michard et al., 1996). They are separated into a lower eclogitic unit (Zermatt-Saas-like) and into an upper blueschist unit (Combin-like). The lower shows many lithostratigraphic and metamorphic similarities with the Zermatt-Saas Unit defined in the northern part and consists of different ophiolitic complexes (e.g. the Orsiera Rocciavrè ophiolites: Pognante, 1979, 1980, 1981; the Monviso ophiolitites: Lombardo et al., 1978; Lardeaux et al., 1987; Philippot, 1988). Likewise, the upper unit is similar to the Combin Unit and is mainly composed of upper Jurassic (De Wever and Caby, 1981) to late Cretaceous calcschists (Lemoine et al., 1984) with subordinated slices of oceanic lithosphere (e.g. Lagabrielle and Lemoine, 1997).

In the Lower Piedmont Zone the occurrence of coesite is reported from the Cignana Unit, in Valtournenche, indicating P of 26-28 kbar and T of 600 °C (Reinecke, 1991, 1998) and similarly Bucher *et al*. (2005) reported. 25-30 kbar at 550-600 °C for the northern Zermatt-Saas Zone. According to Messiga *et al*. (1999) and Schwartz *et al.*, (2000) the Monviso ophiolites reached maximum PT conditions of 19-24 kbar at 580-620 °C. In the central part, Agard *et al.*(2001) reported PT estimations of 450-550 °C and 18-20 kbar for garnet-chloritoid calcschists immediately at the west of the Dora-Maira Massif. Recently, Angiboust et al., (2009) proposed similar PT conditions for the whole Zermatt-Saas Zone in the range 520-560 °C and 22-25 kbar. The greenschist facies metamorphic overprinting developed at 400-475 °C and 4-5 kbar and is mainly concentrated along top to SE shear zones in its northern part (Täschalp region north of the Monte Rosa Massif; Barnicoat *et al*., 1995; Cartwright and Barnicoat, 2002). The HP event is dated at 43-54 Ma (Rb-Sr white mica, Duchêne *et al*., 1997; U-Pb zircon with SHRIMP, Rubatto *et al*., 1998; Rb-Sr and ^{40}Ar-^{39}Ar white mica, Dal Piaz *et al*., 2001; *in situ* ^{40}Ar/^{39}Ar phengite, Agard et al., 2002; Rb-Sr white mica, Cartwright and Barnicoat, 2002; Lu-Hf and Sm-Nd garnet, Lapen et al., 2003; *in situ* ^{40}Ar-^{39}Ar phengite, Gouzu *et al.,* 2006; ^{40}Ar-^{39}Ar white mica Beltrando et al., 2009) while the greenschist re-equilibration spread from 36 to 42 Ma (Rb-Sr whole rock-white mica, Amato *et al*., 1999; Cartwright and Barnicoat, 2002; Beltrando et al., 2009).

In the Upper Piedmont Zone the HP event developed under blueschist facies conditions (12-13 kbar and 425-475 °C in Täschalp region, Cartwright and Barnicoat, 2002; 12-20 kbar and 300-450 °C in the northern Queyras,

Agard et al., 2001; Michard *et al.*, 2003; 8-14 kbat at 300-475 °C in southern Queyras; Tricart and Schwartz, 2006). Age dating is mainly related to the Queyras calcschists: 43-47 Ma in the western sector and 54-65 Ma in the eastern (Agard *et al.*, 2002). The re-equilibration event was developed under greenschist facies conditions (5-9 kbar and 250-450 °C in northern Aosta Valley, Reddy *et al*. 1999; 4-5 kbar and 400-475 °C for shear zones in Täschalp at 37-42 Ma, Cartwright and Barnicoat, 2002; 5-8 kbar and 250-450 °C in the Queyras Agard *et al.*, 2002) during late Eocene (34-39 Ma; Rb-Sr white mica, Inger and Ramsbotham, 1997; Agard et al., 2002).

Lithostratigraphic setting

The study area is located on the left side of the middle Susa Valley where the Upper Polymetamorphic Unit of the Dora-Maira Massif and the Lower Piedmont Zone outcrop. Recent field-survey for the CARG (CARtografia Geologica; new geological maps at 1:50.000 scale) project (Carraro et al., 2002) and for the project of the new Torino-Lione railway (Sacchi et al., 2004) considered the calcschists in contact with the Dora Maira marbles to be in stratigraphic relationship and to be the youngest sediments of the continental Mesozoic cover in agreement with the lithostratigraphy reconstructed by Marthaler et al., (1986) and Tallone, (1988, 1990). These authors reconstructed a monometamorphic cover sequence consisting of impure quartzites (Permian-Lower Triassic), dolomitic marbles (Middle Triassic), grey marbles (Upper Jurassic) and calcschists (Upper Cretaceous) for the northern Dora-Maira Massif.

Careful field work in the study area enhanced the presence of two types of calcschists: (a) subordinate metabasites-free calcschists with grey marbles layers in stratigraphic contact with dolomitic marbles of the Dora-Maira. These calcschists represent the youngest sediments of the Molaras-type sequence (Marthaler et al., 1986; Tallone, 1988, 1990); (b) abundant calcschists in tectonic contact with the dolomitic marbles marked by the presence of mylonites deriving from both rock-types (Fig. 2a) as clearly visible on the South slope of the Monte Molaras. Calcschists (b) contain several bodies of metabasites and of serpentinites (Fig. 2b and Fig. 3) which locally preserve a stratigraphic cover consisting of micaschists and impure marbles. The contact between calcschists (b) and the oceanic crust of the Lower Piedmont Zone is stratigraphic and is marked by basaltic breccias (5-6 m thick; Fig. 2c-d) by altered meta basalts/breccias (amphibole-chlorite-calcite-epidote rich schists in Fig. 2c) and by impure marbles (Fig. 2c) which represents the bottom of the calcschists sequence. At the base of this sequence are present layers (1-4 m thick) of garnet-ankerite micaschists while towards the top are present bodies of metabasites/serpentinites and up to 10 m thick layers of meta-rudstones (meta-conglomerates or meta-

breccias) consisting of marble clasts in a calcite matrix (Fig. 2e) which are interpreted as olistoliths and as debris-flows, respectively. Therefore, calcschists (b) show a strong oceanic affinity which imply and a new interpretation on the structural relationships between the Dora-Maira and the Lower Piedmont Zone that will be discussed later.

According to this new lithostratigraphic setting, in the study area, the Lower Piedmont Zone (Fig. 2f and Fig. 3) shows an overturned sequence made of an oceanic basement of serpentinites and metabasites in stratigraphic contact with heterogeneous calcschists containing (from bottom to top of the stratigraphic sequence) marbles and micaschists layers, metabasites and serpentinites lenses and meta-rudstones suggesting the presence of a basal pelagic sedimentation represented by marbles lying on an heterogeneous oceanic crust followed by a detrital sequence of turbidites (mainly carbonatic), debris flows and slumps probably representing the transition from an ocean-floor to a trench sedimentation. Eclogite facies relic are only found on the eastern side of the Dora-Maira north of Condove (Fig. 1) and are represented by eclogite boudins (Omp + Grt + Gln + Rt) hosted in a foliated matrix recrystallized under greenschist facies conditions, while on the western side are only present scattered Grt + Rt relics. Likewise, Agard et al. (2001) reported PT estimations of 450-550 °C and 18-20 kbar for garnet-chloritoid calcschists west of the Dora-Maira Massif near Colle delle Finestre (Fig. 1).

The Dora-Maira comprises an orthogneisses complex, a polymetamorphic basement and a Mesozoic Cover. The orthogneisses complex is heterogeneous and consists of fine grained flaser gneisses, of augen-gneisses and of aplitic dykes intruded into the basement. The polymetamorphic basement consists of fine to medium-grained garnet ± chloritoid micaschists which locally host metabasite bodies which rarely preserve eclogite facies assemblages. Well preserved eclogites outcrop E of the study area NW of the village of Borgone (Pognante and Sandrone, 1989; see star in in Fig. 1) and are interpreted as metagabbros because of their domain texture consisting of alternating Omp, Zo and Grt rich layers or lenses (Fig. 2g). The Mesozoic Cover is in stratigraphic contact with the polymetamorphic basement or with the orthogneisses complex and consists of discontinuous quartzites and carbonate-bearing micaschists (calc-micaschists) with quartz-rich bands and of thick dolomitic marbles which are overlain by calcschists (a) devoid of metabasites. These calcschists are rather homogeneous consisting of calcite-rich layers alternating to subordinate mica-rich ones (Fig. 2h). The new structural setting we propose for the northwestern Dora-Maira is represented in the geological map of Fig. 3 were the position of the DM *vs* PZ boundary according to Carraro et al. (2002) and Sacchi et al. (2004) is also reported with two red arrows.

Structural evolution

Field mapping on an area of *ca* 7 km^2 and the structural analysis of outcrops with well exposed structures has permitted to distinguish four Alpine tectono-metamorphic events (from pre-D_1 to D_3) followed by a ductile to brittle event (D_4). The study area is marked by a regional foliation concordant with the lithological boundaries, dipping 30-50° W to NW (Fig. 4). The mineral assemblages related to the different deformation events are sketched in Table 1.

Pre-D_1 structures and metamorphism

In the Dora-Maira Massif pre-S_1 foliations and structures are well preserved only within more competent lithologies like dolomitic marbles (Fig. 5a) while in other rock-types they are only preserved in D_1 fold hinges as relic metamorphic foliations (Fig. 5b to e). In marbles pre-D_1 folds are characterized by elongated isoclinal hinges with cusps and lobes morphology and rarely a metamorphic foliation older than pre-D_1 is still preserved (pre-S_{HP} in Fig. 5a). Because dolomitic marbles are almost mono-mineralic rocks with low amount of white mica and chlorite it is not possible to determine the metamorphic facies under which the pre-D_1 surfaces were developed. Despite this, the high Si content of phengite reported by Borghi at al. (2009) for the Foresto (max 3.55 Si a.p.f.u.) and the Chianocco (max 3.75 Si a.p.f.u.) marbles suggests that pre-D_1 crystallized under HP conditions. Pre-D_1 relic surfaces are rarely preserved both in DM metapelites and metabasites and are defined by HP minerals: Wm + Cld + Grt + ChlI + Qtz + Rt in metapelites and Omp + Grt in metabasites. The structural elements related to the pre-D_1 event are only preserved in marbles: fold axes (pre-A_1) mainly consist of intersection lineations defined by oxides and white mica while the stretching lineation (pre-L_1) is mainly defined by the elongation of carbonate grains and of white mica. Both fold axes and pre-L_1 are parallel to each other and are scattered because of the reorientation during the following deformation stages. However, they mainly trend NW-SE (Fig. 4a) with some data plunging towards N to NE.

D_1 structures and metamorphism

The regional foliation S_1 is well developed in all rock types except in the dolomitic marbles that never re-crystallize into a new axial plane foliation in correspondence of the D_1 fold hinges (Fig. 6a). The pre-S_1 in

marbles is transposed parallel to S_1 (compare Fig. 4a-b), therefore, from the structural point of view, pre-S_1 foliations in marbles have the same orientation of the S_1 in other rock-types. Instead, from the metamorphic point of view, pre-S_1 is defined by Phe with high Si content developed under HP conditions (Borghi et al., 2009). In metapelites, orthogneisses and calcschists (both DM and PZ) D_1 folds are isoclinal to rootless (Fig. 5c-d) and the S_1 mainly dips 25-40° towards NNW in the south-eastern part of the study area and 25-45° towards W in the north-western part because of the effect of a major D_3 fold. Instead, the presence of some poles dipping towards S is related to the D_2 deformation phase. Fold axes (A_1) and stretching lineations (L_1) are parallel to each other and plunge mainly 10-45° towards SW to NW (Fig. 4b-c-d). The parallelism between fold axes and stretching lineations suggests the presence of sheath folds which is confirmed by the presence of well preserved anvil-shaped folds (Mies, 1993) within micaschists and orthogneisses (Fig. 5d-e) at the meso-scale and by eye-shaped folds (Mies, 1993) at the macro-scale (Fig. 3). Shear sense indicators consist of σ-shaped Kfs porphyroclasts in orthogneisses and by σ-shaped quartz aggregates within DM calc-micaschists and are consistent with top to W sense of shear (Fig. 5f-g) The D_1 deformation phase is responsible for the lithological repetition of DM dolomitic marbles and PZ calcschists on the southern side of Mt. Molaras (Fig. 5h). The S_1 foliation is defined by greenschist facies assemblages: Wm + Chl + Ab + Qtz + Spn ± green-Am in the PZ metabasites and by Wm + ChlII + Ab + Qtz+ Rt/Ilm in the DM basement.

The tectonic contact between DM and PZ is folded by D_1 isoclinal folds (Figs. 5h and 6a). The mylonitic foliation developed mainly at the expense of PZ calcschists and enveloped stretched boudins of DM marbles. Mylonitic marbles are subordinate and are characterized by strong grain-size reduction. In Fig. 6a the pre-S_1 foliation within DM marbles is cut by the mylonitic foliation and both metamorphic surfaces (pre-S_1 and S_{myl}) are folded by D_1 which developed a regional foliation only in the PZ calcschists and not in DM marbles. The mylonitic foliation along the tectonic contact concordantly shows top to the W sense of shear (Fig. 6b). Locally, slices of DM litho-stratigraphic sequence are present along the tectonic contact and the stratigraphic contact between the DM basement and its Mesozoic cover is decoupled.

D_2 structures

D_2 developed open to close folds and locally shows overturned short limbs (Fig. 6c). The S_2 axial surfaces dip generally towards NNW to N by 25 to 75° with some poles dipping towards S probably because of the presence of box folds (Fig. 4e). A new axial plane foliation occurs discontinuously only in the polymetamorphic

micaschists and is defined by a crenulation cleavage (Fig. 6d). D_2 fold axes generally plunge W to SW by 5-25° with some data plunging NE. The folds asymmetry is concordant with a top to S sense of shear with steep short limbs (see cross sections in Fig. 3).

D_3 structures and late evolution

D_3 is mainly developed at the macro-scale and is responsible for the change in the dip direction of the regional foliation from NNW to W in the sector west of the Monte Molaras. It consists of an antiform fold with an open profile and the axial surfaces dip towards E by 30 to 70° while fold axes trend NNW-SSE with a low inclination. The parasitic folds asymmetry indicate a top to the W sense of shear. This hectometre scale fold deformed the D_2 antiform (marked by a in Fig. 3) re-orienting its axial plane from NNW to W dipping. Some parasitic folds show an axial plane dipping towards SW with an high angle and are indicative of the presence of minor box folds.

The late structural evolution is characterized by the development of the Falcemagna fault zone which dip NNW by 25-40° and is characterized by the presence of mylonites mainly developed at the expense of the dolomitic marbles (Fig. 6e) and of the garnet micaschists. This late structure displaced the main axial plane of the D_3 antiform (marked with black arrows in Fig. 3) and the northern block shows an apparent left-lateral offset of 1 km. However, the absence of well-exposed fault planes with clear shear sense direction did not allow to establish the kinematics with certainty. This mylonitic shear zone grades into frictional regime structures which caused a pervasive fracturing/cementing process in the dolomitic marbles responsible for the development of *cargneoules* which locally are the only evidence for the presence of the Falcemagna fault. Sacchi et al. (2004) have enhanced the parallelism between D_2 axial surfaces and the Falcemagna fault that they considered as a reverse-slip fault. In this work, the parallelism is confirmed, however, the abrupt interruption of the S_3 axial planes in correspondence of the Falcemagna fault (Fig. 3) demonstrates that it was still active after the D_3 deformation phase.

Finally, a discontinuous extensional crenulation cleavage (ECC; *sensu* Platt and Vissers, 1980) developed in the phyllosilicate-rich rocks (Fig. 6f) that evolve into extensional brittle faults mainly in dolomitic marbles (Fig. 6e) with less than 1 m displacement. These late discrete shear zones show top to WSW sense of shear and dip W by 40-60° cutting the Falcemagna fault (Fig. 6e).

Mineral chemistry of Dora-Maira metapelite

Minerals were analyzed with a Cambridge Stereoscan 360 SEM equipped with an EDS Energy 200 and a Pentafet detector (Oxford Instruments). The operating conditions were 15 kV accelerating voltage and 50 s counting time. Mineral formulae were recalculated assuming all measured Fe as FeO. Garnet and chloritoid were recalculated on the basis of 12 oxygens, white mica on the basis of 11 oxygens, feldspar on the basis of 8 oxygens, chlorite on the basis of 28 oxygens, and epidote on the basis of 25 oxygens and assuming Fe_2O_3 = 1.1119*FeO. Mineral abbreviations are given according to Kretz (1983) with the update of Bucher and Frey (2002).

Dora-Maira metapelites consist of fine to medium grained micaschists often characterized by lenticular aggregates or layers of Qtz or Wm which define a compositional layering. In correspondence of D_1 fold hinges a pre-S_1 foliation defined by of Phe + Pg + Cld + ChlI + Grt + Qtz + Rt (M1 assemblage) is preserved. This HP foliation is generally overprinted by the regional S_1 foliation defined by Ms + Pg + ChlII + Ab + Qtz + Ilm ± Bt (M2 assemblage).

Sample SU5 is a Grt-Cld bearing micaschists of the Dora-Maira polymetamorphic basement and was collected 7 km east of the study area (Fig. 3) close to eclogite body studied by Pognante & Sandrone (1989). It shows a pre-S_1 HP foliation preserved in rootless fold hinges (Fig. 7a-b-d-e) and is defined by alternating Qtz-rich and Wm-rich millimetric layers and by the PDO of Phe + Pg + Cld + ChlI + Qtz + Rt in textural equilibrium with the rim. The micaschist is characterized by a bimodal distribution of Grt size, particularly GrtI has dimensions > 1 mm while GrtII rarely exceed 500 μm. Both garnet types preserve an inclusion-rich core which locally preserves an internal foliation defined by Ilm (Fig. 7c). The inclusions in Grt core consists of Qtz + Ilm and of elongated aggregates of Rt interpreted as pseudomorphs after former Ilm. In this sample the re-equilibration stage (M2 assemblage) is poorly developed and is represented by Ms + ChlII + Ilm which developed around Phe, at the expense of Cld + Grt and at the rim of Rt, respectively. Representative minerals chemistry is reported in Table 2.

Garnet

GrtI has up to 2 mm dimensions (Fig. 7a-c-f), include Qtz + Ilm (locally replaced by Rt aggregates) + Rt and preserve a discrete growth zoning that reveals the presence of four different chemical compositions (core, mantle I, mantle II, rim; Fig. 7f). The presence of four different growth shells is strongly displayed by Ca and Fe X-rays

maps (Figs. 7g-h) which also enhance a Grs increase in the outer core. GrtII has smaller dimensions (max 500-600 μm) but shows the same compositional zoning of GrtI (Fig. 8a-b-c) suggesting the presence of a single garnet generation. In fact, the garnet bimodal distribution cannot be justified only by the fact that some garnet are not sectioned trough the core. Moreover, the Grt dimensions strongly depend on the volume of the core suggesting that it could be an inherited one. Both GrtI and GrtII are characterized by a flat core, a mantle which shows a Grs-enrichment coupled to a decrease in Alm content and a rim showing increasing Alm and decreasing Grs (Fig. 8a to d). The Prp content slightly increases from core to mantle I and then decreases towards the rim while the Sps amount decreases towards the rim and MnO is all stored in the garnet core. The four different compositions are: $Alm_{79-83}Grs_{7-9}Prp_{5-7}Sps_{4-9}$ (core), $Alm_{70-73}Grs_{19-24}Prp_{6-8}$ (mantle I), $Alm_{77-80}Grs_{14-17}Prp_{5-7}$ (mantle II) and $Alm_{85-87}Grs_{7-8}Prp_{4-6}Sps_{0-2}$ (rim). The XMg increases from core (0.06-0.07) to mantleI (0.08-0.09) and then decreases again at mantle II (0.07-0.08) and rim (0.06). The garnet zoning and morphology, characterized by a large core, are similar to that investigated by Le Bayon et al. (2006) for a polymetamorphic Grt-Cld micaschists in the northern part of the Gran Paradiso Massif. Therefore, also the core of the garnet in the studied sample can represent a pre-Alpine relic. This hypothesis is confirmed by the presence of inclusions in the Grt core consisting of Qtz + Ilm + Gr which locally define an internal foliation (Fig. 7c).

White mica

White mica is represented mainly by medium-grained Phe in textural equilibrium with rare Pg. This Phe locally shows a thin rim of Ms. Phengite shows some core with up to 3.55 Si a.p.f.u. while the rim contains around 3.20-3.35 Si a.p.f.u. (Fig. 8e) coupled to decreasing XMg from core (0.70-0.72) to rim (0.50-0.52) and rather constant XNa around 0.05-0.10. Ms is unzoned with 3.05-3.17 Si a.p.f.u., 0.39-0.49 XMg and 0.15-0.22 XNa. Finally, Pg contains up to 0.09 K a.p.f.u. According to textural relationships, the Ms is linked to re-crystallization mainly in correspondence of D_1 rootless folds.

Other minerals

Chloritoid has up to 350 μm dimensions, often is in aggregates and is always associated to Phe. Cld is unzoned with constant XMg 0.13-0.17 and shows a constant deficiency in Al in the range of 0.02-0.12 a.p.f.u. which is indicative of the presence of a little amount of Fe^{3+} which contributes to enlarge the $XMg_{(Fe2+)}$ to 0.13-0.18. ChlI

is rare and defines the pre-S_1 foliation while ChlII is abundant and consists of fine-grained aggregates at the expense of Grt or Cld. Both generations shows constant XMg around 0.36-0.42 and are ripidolite in composition (Fig. 8f).

Metamorphic evolution

The pseudosection was calculated in the system NCKMFASH with Perple_X (Connolly, 1990; Connolly & Petrini, 2002) using the thermodynamic database of Holland & Powell (1998, 2002 update). All Fe was considered as ferrous and H_2O was used as a saturated pure fluid-phase (i.e. $aH_2O=1$). This is a realistic assumption for the studied samples since they contain abundant hydrous phases and because of the absence of carbonates and sulphides. The following solid solution models have been used: biotite (Tajcmanova et al., 2009), garnet (White et al., 2007), clinopyroxene (Green et al., 2007), feldspar (Holland & Powell, 2003), paragonite (Chetterjee & Froese, 1975), phengite-muscovite, chlorite, talc, chloritoid, staurolite and carpholite (Holland & Powell, 1996, 1998). Capital letters indicate solid solution models and small letters indicate pure phases; fields of di-, tree-, quadri- and penta-variant mineral assemblages are represented from white to dark grey hues.

The garnet core is not important for the aim of this paper because is a pre-Alpine relic and therefore is not investigated with pseudosection modelling. However, it strongly contributes to the fractionation of the rock bulk composition since represent a big volume of the whole garnet present in this sample. The Grt core composition was fractionated according to the method of Gaidies et al., (2006) and was subtracted from the bulk XRF composition performed at the Vancouver laboratories of the ALS Chemex. The composition used for pseudosection modelling are reported in Table 3.

Since Grt mantleI has no detectable MnO it is not possible to apply the methods of Gaidies et al. (2006) to fractionate its composition and therefore the bulk composition of column B (Table 3) is used to calculate the PT conditions for both mantleI and mantleII. According to Fig. 7f-g-h, the vol. % amount of Grt mantleI is low and its fractionation barely changes the effectively reacting bulk composition.

Pseudosection of Fig. 9 is contoured for Grs content and XMg in Grt and Si a.p.f.u. in Phe (Fig. 9b), for XMg and vol. % of Cld (Fig. 9c) and Chl (Fig. 9d), respectively. The mantle I (0.08-0.09 XMg, Grs_{19-24}) to mantle II (0.07-0.08 XMg, Grs_{14-17}) garnet compositions registered a decompressional heating from *ca* 515 °C at 19-20 kbar to *ca* 560 °C at 10-11 kbar in the Chl + Cld + Phe + Pg + Grt + Qtz stability field (M1 assemblage). No intersection was observed for Grt rim composition probably because the bulk-chemical composition is not

relevant for its growing conditions or because it represents a re-equilibration stage. The decompressional heating path is compatible with Grt growth since in this field assemblage it is the only Ca-bearing phase and the garnet content increases with decreasing Grs content at increasing T. Along this PT path the Si content in Phe decreases from 3.40 to 3.15 a.p.f.u. while the maximum content measured (3.55 Si a.p.f.u.) is not modelled in this PT range probably representing the relic of a prograde foliation or of an higher P stage. During decompression Cld is consumed and at peak-pressure the calculated composition (XMg 0.20-0.22) is slightly Mg enriched compared to that measured (XMg 0.13-0.18) which instead is compatible with a prograde path during Cld growth. Indeed, Cld grew along the prograde path with a composition in the range 0.13-0.18 up to 19 kbar from were it should grow very little with a Mg-richer composition. Since the pre-S_1 foliation is defined by Cld it represents a prograde foliation up to the peak pressure conditions developed at 515 °C and 19-20 kbar. Instead, ChlI mainly grew on decompression and the calculated composition should be 0.50-0.54 XMg at peak-P (3-5 vol. %) and 0.44-0.46 at 10-11 kbar (8-9 vol. %) while the measured one is 0.36-0.42 XMg. Such a Fe-rich Chl is stable only at T < 550-575 °C and P < 10-11 kbar. The reasons for the discrepancy between calculated and measured Chl composition is related to the complete re-equilibration of ChlI at lower PT conditions or could be due to the fractionation effect of other Fe-Mg minerals such as garnet, phengite and chloritoid. Finally, since Grt mantle II is stable down to *ca* 575 °C at 7-8 kbar, the possibility that it continued to grow out of the Cld stability field cannot be ruled out (dashed line in Fig. 9d).

Discussions

In the study area the pre-D_1/M1 tectono-metamorphic stage is well preserved within metapelites (Cld-bearing foliations). It occurred under eclogite facies conditions at 18-20 kbar and 510-520 °C and is characterized by the assemblage Cld + Grt + Phe + Pg + Qtz + ChlI + Rt in the basement micaschists. In the northern portion of the Dora-Maira Massif PT conditions of 10-15 kbar and 450-550 °C (Borghi et al., 1985, Pognante and Sandrone, 1989; Cadoppi, 1990; Chopin et al., 1991, Borghi et al., 1996) are reported for the same tectonic unit studied in this work which are lower than that reported here but were retrieved by classical thermobarometry. Moreover, the presence of Phe core with up to 3.55 Si a.p.f.u. can represent the relic of an older metamorphic stage at higher P than that estimated (18-20 kbar) since at these conditions Phe should contain only 3.40 Si a.p.f.u. according to pseudosection modelling. This hypothesis is corroborated by the high Si content in Phe (3.55-3.75 Si a.p.f.u.) of the Dora-Maira marbles reported by Borghi et al., (2009).

The continuous garnet growth in metapelites during decompression registered a prograde decompressional heating to 550-560 °C at 10-11 kbar that can be considered as a growth stage developed in continuity with pre-D_1/M1 stage. The garnet rim composition shows no intersection in Fig. 9b probably because the pseudosection was calculated without MnO which extend the Grt stability towards lower PT conditions. However, the Grt rim composition shows an Alm enrichment coupled to Grs decrease and should represent a further decompression just before the re-equilibration under greenschist facies conditions. The D_1/M2 tectono-metamorphic stage developed syn-kinematically with respect to the regional foliation S_1 during top to the W shearing and is defined by the assemblage Ms + Pg + ChlII + Qtz + Ab + Rt/Ilm. Pseudosection modelling of metapelite sample (Fig. 9) suggests that D_1/M_2 developed at P < 7 kbar and T < 575 °C which thus represent max PT conditions for the greenschist facies re-equilibration.

The reconstructed PT path (Fig. 10) shows a clockwise trajectory, characterized by an inferred prograde stage along a 7°C/km geothermic up to the eclogitic peak (M1 stage). The exhumation path shows a decompression of at least 10-13 kbar (35-45 km of exhumation) linked to a maximum heating of 50-60 °C then followed by the development of the main regional tectono-metamorphic event (M2). Therefore, the S_1 foliation equilibrated in a geodynamic setting characterized by an apparent geothermic gradient major than 20-25 °C/km.

The Alpine PT path presented in this work is different from that reported by Borghi et al., (1996) and is very similar to the PT path reconstructed by Le Bayon et al., (2006) for the northern Gran Paradiso Massif on the basis on pseudosection modelling of a Grt-Cld bearing micaschist (Fig. 10).

Along the tectonic contact between the Dora-Maira marbles and the Piedmont Zone calcschists the geometric relationships between the different generations of metamorphic foliations suggest that these two units were coupled after the pre-S_1/M1 eclogite facies stage and before the development of S_1/M2 regional foliation under greenschist facies conditions (Fig. 6a). The tectonic contact between the Dora-Maira and the Lower Piedmont Zone is deformed by the D_1 event (Fig. 3) which developed meso to macro-scale non cylindrical folds as also suggested by the parallelism between L_1 and D_1 fold axes and took place during widespread top to the W non coaxial shearing. Therefore, the Dora-Maira was coupled to the Lower Piedmont Zone during exhumation along the subduction channel probably just before the development of the regional foliation since along the tectonic contact the eclogite facies assemblages are completely erased suggesting nappe coupling at lower PT conditions than the eclogite facies (< 12-13 kbar *ca*).

Geochronological data for the northern Dora-Maira lack and the age dating of the UHP metamorphism in the southern part of the massif (Gebauer et al., 1997) cannot be extrapolated to the northern one since the tectono-

metamorphic evolution is strongly different. Therefore, no speculation can be undertaken regarding the exhumation rate for the study area and for the Upper Polymetamorphic Unit of the Dora-Maira Massif in general.

Conclusions

Detailed field mapping has permitted to re-interpret the position of the tectonic contact between the Dora-Maira Massif and the Piedmont Zone along the middle Susa Valley. It is not a flat lying contact gently deformed around the Dora-Maira dome as drawn in the previous work (Carraro et al., 2002, Sacchi et al., 2004) but it is isoclinally folded by the D_1 deformation stage responsible for the development of the regional foliation in this area. The reconstruction of the lithostratigraphy of the Dora-Maira Mesozoic cover has shown that the Upper Cretaceous calcschists of the previous works (Marthaler et al., 1986; Tallone, 1988, 1990) consist of subordinate ophiolite-free calcschists in primary contact with the dolomitic marbles and mainly of ophiolite bearing carbonatic metasediments in primary contact with the oceanic lithosphere.

This new lithostratigraphic setting and the reconstruction of the metamorphic evolution allowed to infer that the Dora-Maira Massif and the Piedmont Zone were coupled during exhumation after the M1/pre-S_1 (eclogite facies conditions) and before the M2/S_1 (greenschist to amphibolite facies conditions) tectono-metamorphic stages.

The northern Dora-Maira Massif registered an eclogite facies peak pressure at 18-20 kbar and 515-525 °C (M1 stage and pre-S_1 foliation) and then was exhumed during increasing T (10-11 kbar and 555-565°C). The M2 assemblage defining the S_1 regional foliation developed at $P < 7$ kbar and $T < 575$ °C. According to the structural evolution and to petrological investigation we suggest that the Dora-Maira Massif and the Piedmont Zone were coupled in the lower to medium crust along the subduction channel during their exhumation between 7-12 kbar.

Finally, the tectono-metamorphic evolution reconstructed for northern Dora-Maira vs Piedmont Zone boundary is similar to that reported by Gasco et al., (2009) for the eastern Gran Paradiso vs Piedmont Zone boundary. This strongly suggest that the Internal Crystalline Massifs shared a similar tectono-metamorphic evolution during the post-eclogitic exhumation at which time they were coupled to the oceanic lithosphere of the Piedmont Zone.

Acknowledgments. This work was financially supported by Ministero dell'Università e della Ricerca Scientifica e Tecnologica (M.U.R.S.T.).

References

Agard, P., Monié, P., Jolivet, L., Goffé, B., (2002). Exhumation of the Schistes Lustrés complex: in situ laser probe $^{40}Ar/^{39}Ar$ constraints and implications for the Western Alps. Journal of Metamorphic Geology, 20, 599-618.

Agard, P., Vidal, O., Goffé, B., (2001). Interlayer and Si content of phengite in HP-LT carpholite-bearing metapelites. Journal of Metamorphic Geology, 19, 479-495.

Amato, J.M., Johnson, C.M., Baumgartner, L.P., Beard, B.L. (1999). Rapid exhumation of the Zermatt-Saas ophiolite deduced from high-precision Sm-Nd and Rb-Sr geochronology. Earth and Planetary Science Letters, 171, 425-438.

Angiboust, S., Agard, P., Jolivet, L., Beyssac, O., (2009). The Zermatt-Saas ophiolite: the largest (60-km wide) and the deepest (c. 70-80 km) continuous slice of oceanic lithosphere detached from a subduction zone? Terra Nova, 21, 171-180.

Avigad, D., Chopin, C., Goffe, B., Michard, A., (1993). Tectonic model for the evolution of the western Alps. Geology, 21, 659-662.

Bearth, P., (1967). Die Ophiolithe der Zone von Zermatt–Saas Fee. Beiträge Geologische Karte Schweizerische, Neue Folge 132, 1–130.

Borghi, A., Cadoppi, P., Porro, A., Sacchi, R., Sandrone, R., (1984). Osservazioni geologiche nella Val Germanasca e nella media Val Chisone (Alpi Cozie). Bollettino del Museo di Scienze Naturali, Torino, 2, 503-530.

Borghi, A., Cadoppi, P., Porro, A., Sacchi, R., (1985). Metamorphism in the northern part of the Dora Maira Massif (Cottian Alps). Bollettino del Museo Regionale di Scienze Naturali, Torino, 3, 369-380.

Borghi, A., Compagnoni, R., Sandrone, R. (1996). Composite P-T paths in the internal Penninic massifs of the western Alps: Petrological constrains to their thermo-mechanical evolution. Eclogae Geologicae Helvetiae, 89, 345–367.

Borghi, A., Vaggelli, G., Marcon, C., Fiora, L., (2009). The Piedmont white marbles used in antiquity: an archaeometric distinction inferred by a minero-petrographic and C-O stable isotope study. Archaeometry, 51, 913-931.

Bucher, K., Fazis, Y., De Capitani, C., Grapes, R., (2005). Blueschists, eclogites, and decompression assemblages of the Zermatt-Saas ophiolite: high-pressure metamorphism of subducted Tethys lithosphere. American Mineralogist, 90, 821–835.

Bucher, K., Frey, M., (2002). Petrogenesis of Metamorphic Rocks. Springer-Verlag, 7th edition, p. 335-336.

Bussy, F., Cadoppi, P., (1996). U-Pb zircon dating of granitoids from the Dora-Maira massif (western Italian Alps). Schweizerische Mineralogische und Petrographische Mitteilungen, 76, 217-233.

Cadoppi, P., (1990). Geologia del basamento cristallino nel settore settentrionale del Massiccio Dora-Maira (Alpi Occidentali). PhD thesis, University of Torino, 208 pp.

Caron, J.M. (1977). Lithostratigraphie et tectonique des Schistes Lustrés dans les Alpes Cottiennes septentrionales et en Corse orientale. Mémoire de Science Géologique, Strasbourg, 48, 326 pp.

Carraro, F., Cadoppi. P., Castelletto, M., Sacchi, R., Baggio, P., Giraud, V., Bellardone, G., (2002). Note illustrative della carta geologica d'Italia alla scala 1:50.000, Foglio 154 Susa. Servizio Geologico

d'Italia, 123 pp.

Cartwright, I. Barnicoat, A.C. (2002). Petrology, geochronology, and tectonics of shear zones in the Zermatt-Saas and Combin zones of the Western Alps. Journal of Metamorphic Geology, 20, 263-281.

Chatterjee, N.D., Froese, E., (1975). A thermodynamic study of the pseudobinary join muscovite-paragonite in the system $KAlSi_3O_8$–$NaAlSi_3O_8$–Al_2O_3–SiO_2–H_2O. American Mineralogist, 60, 985-993.

Chopin, C., (1984). Coesite and pure pyrope in high-grade blueschist of the Western Alps: a first record and some consequences. Contributions to Mineralogy and Petrology, 86, 107-118.

Chopin, C., Henry, C., Michard, A., (1991). Geology and petrology of the coesite-bearing terrain, Dora Maira massif, Western Alps. European Journal of Mineralogy, 3, 263– 291.

Compagnoni, R., Hirajima, T., Turello, R., (1993). L'unità a coesite di Brossasco-Isasca, Massiccio Dora-Maira meridionale, Alpi Occidentali. 60° Congresso SIMP, Torino, Guida all'escursione, Plinius, 10, 275-293.

Connolly, J.A.D., (1990). Multivariable phase diagrams: an algorithm based on generalized thermodynamics. American Journal of Science, 290, 666-718.

Connolly J.A.D., Petrini K. (2002). An automated strategy for calculation of phase diagram sections and retrieval of rock properties as a function of physical conditions. Journal of Metamorphic Geology, 20, 697-708.

Dal Piaz, G.V., (1974). Le métamorphisme alpin de haute pression et basse température dans l'évolution structurale du bassin ophiolitique alpino-appenninique. 1^{e} Partie: Bollettino della Società Geologica Italiana, 93, 437-468, 2^{e} Partie: Schweizerische Mineralogische und Petrographische

Mitteilungen, 54, 399-424.

Dal Piaz, G.V., (1999). The Austroalpine-Piedmont nappe stack and the puzzle of Alpine Tethys. Memorie di Scienze Geologiche, 51/1, 155-176.

Dal Piaz G.V., Cortiana, G., Del Moro, A., Martin, S., Pennacchioni, G. & Tartatotti, P. (2001). Tertiary age and paleostructural inferences of the eclogitic imprint in the Austroalpine outliers and Zermatt-Saas ophiolite, Western Alps. Journal of Earth Sciences, 90, 668-684.

Dal Piaz, G.V., Ernst, W.G., (1978). Areal geology and petrography of eclogites and associated metabasites of the Piedmont ophiolite nappe, Breuil-St. Jacques area, Italian Western Alps. Tectonophysics, 51, 99-126.

De Wever, P., Caby, R., (1981). Datation de la base des schistes lustrés post-ophiolitiques par des radiolaires (Oxfordien- Kimmeridgien moyen) dans les Alpes Cottiennes (Saint Véran, France). Comptes Rendus de l'Académie Des Sciences, Paris, 292, 467–472.

Duchene, S., Lardeaux, J.M. Albaréde, F. (1997). Exhumation of eclogites: insights from depth-time path analysis. Tectonophysics, 280, 125-140.

Gasco, I, Gattiglio, M., Borghi, A., (2009). Structural evolution of different tectonic units across the Austroalpine-Penninic boundary in the middle Orco Valley (Western Italian Alps). Journal of Structural Geology, 31, 301-314.

Gaidies, F., Abart, R., De Capitani, C., Schuster, R., Connolly, J.A.D., Reusser E. (2006). Characterization of polymetamorphism in the Austroalpine basement east of the Tauern Window using garnet isopleth thermobarometry. Journal of Metamorphic Geology, 24, 451-475.

Gebauer, D., Schertl, H.P., Brix, M., Schreyer, W., (1997). 35 Ma old ultrahigh-pressure metamorphism and evidence for very rapid exhumation in the Dora Maira Massif, Western Alps. Lithos, 41, 5-24.

Green, E.C.R., Holland, T.J.B., Powell, R., (2007). An order-disorder model for omphacitic pyroxenes in the system jadeite-diopside-hedenbergite-acmite, with applications to eclogite rocks. American Mineralogist, 92, 1181-1189.

Henry, C., Michard, A., Chopin, C., (1993). Geometry and structural evolution of ultra- high-pressure and high-pressure rocks from the Dora-Maira massif, western Alps, Italy. Journal of Structural Geology, 15, 965-981.

Holland, T.J.B., Powell, R., (1996). Thermodynamics of order-disorder in minerals II. Symmetric formalism applied to solid solutions. American Mineralogist, 81, 1425-1437.

Holland, T.J.B., Powell, R., (1998). An internally consistent thermodynamic data set for phases of petrologic interest. Journal of Metamorphic Geology, 16, 309-343.

Holland, T.J.B., Powell, R., (2003). Activity–composition relations for phases in petrological calculations: an asymmetric multicomponent formulation. Contributions to Mineralogy and Petrology, 145, 492-501.

Inger, S., Ramsbotham, W., (1997). Syn-convergent exhumation implied by progressive deformation and metamorphism in the Valle dell'Orco transect, NW Italian Alps. Journal of the Geological Society of London, 154, 667-677.

Kassem, O.K., Ring, U. (2004). Underplating-related finite-strain patterns in the Gran Paradiso massif, Italian Western Alps: Heterogeneous ductile strain superimposed on a nappe stack. Journal of the Geological Society, London, 161, 875-884.

Kretz, R., (1983). Symbols for rock-forming minerals. American Mineralogist, 68, 277-279.

Lagabrielle, Y., Lemoine, M., (1997). Alpine, Corsican and Apennine ophiolites: the slow-spreading

ridge model. Comptes Rendus de l'Academie Des Sciences, 325, 909–920.

Lapen, T.J., Johnson, C.M, Baumgartner, L.P., Dal Piaz, G.V., Skore, S., Beard, B., (2007). Coupling of oceanic and continental crust during Eocene eclogite-facies metamorphism: evidence from tha Monte Rosa nappe, western Alps. Contributions to Mineralogy and Petrology, 153, 139-157.

Lapen, T.J., Johnson, C.M., Baumgartner, L.P., Mahlen, N.J., Beard, B.L., Amato, J.M. (2003). Burial rates during prograde metamorphism of an ultra-high-pressure tarrane: an example from Lago di Cignana, western Alps, Italy. Earth and Planetary Science Letters, 215, 57-72.

Lardeaux, J.M., Nisio, P., Boudeulle, M., (1987). Deformational and metamorphic history at the Lago Superiore area of the Monviso ophilitic complex (Italian Western Alps). Ofioliti, 12, 479– 502.

Le Bayon, B., Pitra, P., Ballèvre, M., Bohn, M., (2006). Reconstructing P-T paths during continental collision using multi-stage garnet (Gran Paradiso nappe, Western Alps). Journal of Metamorphic Geology, 24, 477-496.

Lemoine, M., Marthaler, M., Caron, J. M. et al., (1984). Découverte de foraminifères planctoniques du Crétacé supérieur dans les schistes lustrés du Queyras (Alpes occidentales). Conséquences paléogéographiques et tectoniques. Comptes Rendus de l'Academie Des Sciences, Paris, 229, 727–732.

Lemoine, M., Tricart, P., (1986). Les Schistes Lustrés piémontais des Alpes Occidentales: Approche stratigraphique, structurale et sedimentologique. Eclogae Geologicae Helvetiae, 79(2), 271-294.

Lombardo, B., Nervo, R., Compagnoni, R., Messiga, B., Kienast, J.R., Mevel, C., Fiora, L., Piccardo, G., Lanza, R., (1978). Osservazioni preliminari sulle ofioliti metamorfiche del Monviso (Alpi occidentali). Rendiconti della Società Italiana di Mineralogia e Petrologia,. 34, 253-305.

Marthaler, M, Fudral, S., Deville, E., Rampnoux, J.P., (1986). Mise en évidence du Crétacé supérieur

dans la couverture septentrionale de Dora-Maira, région de Suse, Italie (Alpes occidentales). Conséquences paléogéographiques et structurales. Comptes Rendus de l'Académie des Sciences Paris, 302, Série II, 91-96.

Messiga, B., Kienast, J. R., Rebay, G., Riccardi, M.P., Tribuzio, R., (1999). Cr-rich Magnesio-Chlorithoid from the Monviso ophiolites (Western Alps, Italy). Journal of Metamorphic Geology, 17, 287-299.

Michard, A., (1967). Etudes géologiques dans les zones internes des Alpes cottiennes. Editions du CNRS, Paris, 448 pp.

Michard, A., Chopin, C., Henry, C., (1993). Compression versus extension in the exhumation of the Dora-Maira coesite-bearing unit, Western Alps. Tectonophysics, 221, 173-193.

Michard, A., Goffé, B., Chopin, C., Herny, C., (1996). Did the Western Alps develop through an Oman-Type stage? The geotectonic setting of high-pressure metamorphism in two contrasting Tethyan transects. Eclogae Geologicae Helvetiae, 89, 43-80.

Michard, A., Avigad, D., Goffé, B., Chopin, C., (2003). The high-pressure metamorphic front of the south Western Alps (Ubaye-Maira transect, France, Italy). Schweizerische Mineralogische und Petrographische Mitteilungen**,** 84, 215–235.

Mies, J.W. (1993). Structural analysis of sheath folds in the Sylacauga Marble Group, Talladega slate belt, southern Appalachians. Journal of Structural Geology, 15, 983-993.

Philippot, P., (1988). Deformation et éclogitisation progressives d'une croûte océanique subductée: le Monviso, Alpes occidentales. Constraintes cinématiques durant la collision Alpine. PhD, Univ. Montpellier I, 230 pp.

Platt, J.P., Vissers R.L.M., (1989). Extensional structures in anisotropic rocks. Journal of Structural

Geology, 2, 397-410.

Pleuger, J., Froitzheim, N., Jansen, E., (2005). Folded continental and oceanic nappes on the southern side of Monte Rosa (western Alps, Italy): Anatomy of a double collision suture. Tectonics, 24, TC4013, doi:10.1029/2004TC001737.

Pognante, U. (1979). The Orsiera-Rocciavrè metamorphic complex (Italian Western Alps). Ofioliti, 4, 183-198.

Pognante, U. (1980). Preliminary data on the Piemonte ophiolite nappe in the lower Val Susa-Val Chisone area, Italian Western Alps. Ofioliti, 5, 221-240.

Pognante, U. (1981). Magmatic and metamorphic evolution of two Fe-Ti gabbroic series from the Piemonte ophiolite nappe in the Susa valley area, Italian Western Alps. Memorie di Scienze Geologiche, Padova, 35, 21-34.

Pognante, U., Sandrone, R., (1989). Eclogites in the Northern Dora-Maira Nappe (Western Alps, Italy). Mineralogy & Petrology, 40, 57-71.

Reinecke, T., (1991). Very-high-pressure metamorphism and uplift of coesite bearing metasediments from the Zermatt-Saas zone, Western Alps. European Journal of Mineralogy., 3, 7-17.

Reinecke, T., (1998). Prograde high- to ultrahigh-pressure metamorphism and exhumation of ocenaic sediments at Lago di Cignana, Zermatt-Saas Zone, Western Alps. Lithos, 42, 147-189.

Rubatto, D., Gebauer, D., Fanning, M., (1998). Jurassic formation and Eocene subduction of the Zermatt-Saas-Fee ophiolites: implications for the geodynamic evolution of the Central and Western Alps. Contributions to Mineralogy and Petrology, 132, 269-287.

Sacchi, R., Balestro, G., Cadoppi, P., Carraro, F., Delle Piane, L., Di Martino, L., Enrietti, M., Gallarà, F.,

Gattiglio, M., Martinotti, G., Perello, P., (2004). Studi geologici in Val di Susa finalizzati ad un nuovo collegamento ferroviario Torino-Lione. Monografie Museo Regionale di Scienze Naturali, Regione Piemonte,Torino, XLI, 117 pp.

Sandrone, R., Cadoppi, P., Sacchi, R., Vialon, P., (1993). The Dora-Maira Massif. In: von Raumer, J.F., Neubauer, F. (Eds.)., Pre-Mesozoic Geology in the Alps. Springer Verlag, Berlin, pp. 317–325.

Schmid, S.M., Fügenschuh, B., Kissling, E., Schuster, R., (2004). Tectonic map and overall architecture of the Alpine orogen. Eclogae Geologicae Helvetiae, 97, 93–117.

Tajcmanova, L., Connolly, J.A.D., Cesare, B., (2009). A thermodynamic model for titanium and ferric iron solution in biotite. Journal of Metamorphic Geology, 27, 153-165.

Tallone, S., (1988). Osservazioni litostratigrafiche e strutturali nella copertura del Massiccio Dora-Maira lungo il fianco sinistro della Valle di Susa. Rendiconti della Società Geologica Italiana, 11, 171-174.

Tallone, S., (1990). Il Dora-Maira settentrionale e le sue coperture mesozoiche: relazioni tra litostratigrafia, struttura ed evoluzione metamorfica. PhD thesis, University of Torino, 147 pp.

Tricart, P., Schwartz, S., (2006). A north-south section across the Queyras Schistes lustrés (Piedmont zone,Western Alps): Syn-collision refolding of a subduction wedge. Eclogae Geologicae Helvetiae , 99, 429-442.

Vialon, P., (1966). Etude géologique du massif cristallin Dora Maira, Alpes cottiennes internes, Italie. Thesis d'Etat, Université de Grenoble, Grenoble, 293 pp.

White, R. W., Powell, R., Holland, T. J. B., (2007). Progress relating to calculation of partial melting equilibria for metapelites. Journal of Metamorphic Geology, 25, 511-527.

Figures captions

Fig. 1 Simplified geological map of the northern Dora-Maira Massif and surrounding units (redrawn after Sandrone et al., 1993; Carraro et al., 2002). The box in b) shows the study area of Fig. 3.

Fig. 2 Main rock types in the Piedmont Zone (PZ) and Dora-Maira Massif (DM): a) tectonic contact between DM marble and PZ calcschists marked by mylonitic rocks developed at the expense of both rock types; b) PZ calcschists with metabasite boudins; c) overturned stratigraphic contact between PZ basaltic breccias and the calcschists marked by the presence of altered metabasites; d) basaltic breccias consisting of fine-grained metabasite clasts in a medium-grained matrix consisting of Chl + Act + Ab + Wm; e) meta-rudstones consisting of stretched marble clasts in a calcite matrix; f) detailed sketch of the lithostratigraphic sequence of the Lower Piedmont Zone south of Chiamberlando-Mt. Molaras; g) eclogite facies metagabbro with a well preserved HP foliation within the DM micaschists, the inset shows the preserved magmatic structure and the eclogitic foliation on a polished slab; h) isoclinally folded Dora-Maira calcschists characterized by alternating calcite-rich (dark grey) and subordinate mica-rich (brown) layers.

Fig. 3 Geological map and cross sections of the study area.

Fig. 4 Equal area projection, lower hemisphere of the main structural features characterizing the four deformation phases identified in the middle Susa Valley.

Fig. 5 Meso-structures representing pre-D_1 and D_1 deformation phases: a) pre-S_1 cusps and lobes fold within DM marbles preserving an older foliation termed pre-S_{HP}; b) pervasive S_1 foliation within Grt-Cld micaschists preserving a pre-S_1 foliation defined by alternating quartz-rich and mica-rich layers; c) D_1 folds in garnet-micaschists inter-bedded within PZ calcschists; d-e) anvil-shaped folds (Mies, 1993) within DM Grt-Cld micaschists related to the development of sheath folds during D_1; f-g) top to W sense of shear in orthogneisses and calc-micaschists of the Dora-Maira Massif, respectively; h) lithological repetition of the DM marbles (M-

DM) and the PZ calcschists (Cs-PZ) at the macro-scale on the southern side of the Mt. Molaras.

Fig. 6 Structural relationships between the DM and the PZ: a) the pre-S_1 foliation within DM marbles is cut by the mylonitic foliation developed mainly at the expense of PZ calcschists. The mylonites are folded by D_1 which developed a regional foliation only in the PZ calcschists and not in DM marbles; b) mylonitic foliation at the expense of PZ calcschists showing top to W sense of shear. Meso-structures representing D_2 and D_3 deformation phases: c) D_2 fold within DM dolomitic marbles with a short overturned limb. The black arrows show the dip direction of the S_2 axial surface towards N with a low angle; d) stratigraphic contact between Grt-Cld micaschists and cover calc-micaschists showing a well-developed S_2 crenulation cleavage only in the basement rocks; e) carbonatic mylonites along the Falcemagna fault displaced by a late normal fault; f) extensional crenulation cleavage developed in fine-grained orthogneisses showing 2-3 cm displacement in the aplitic dike.

Fig. 7 Microstructures of sample SU5: a-b) pre-S_1 foliation preserved as rootless folds in D_1 fold hinges, the box in a is enlarged in b; c) GrtI preserving an internal foliation defined by Ilm interpreted as pre-Alpine; d) pre-S_1 foliation defined by Phe + Cld + ChlI. Cld is partly overgrown by ChlII and Phe (brighter) shows a rim of Ms (darker); e) pre-S_1 foliation defined by Phe + ChlI (medium-grained) and GrtII partly overgrown by ChlII (fine-grained); f) GrtI preserving a complex growth zoning represented in Fig 8a. The inset shows a particular of the rim showing that it is composed of two distinct growth shells which composition is represented in Fig. 8b; g-h) Ca and Fe X-rays map, respectively, showing the presence of four different growth shells.

Fig. 8. Minerals chemistry of sample SU5. a) chemical zoning rim-to-rim profile of GrtI; b) close spaced profiles of GrtI mantle-rim; c) rim-to-rim profile of GrtII showing a similar composition to GrtI; d) core to rim chemical composition of garnet; e) chemical composition of white mica consisting mainly of Phe, minor Ms and Pg; f) chemical composition of ChlI and ChlII.

Fig. 9 a) PT pseudosection for Grt mantle growing conditions after subtraction of the Grt core using composition in column B reported in Table 3; b) contours intersection for Grt mantle I and mantle II compositions; c) XMg and vol. % of Cld; d) XMg and vol. % of Chl.

Fig. 10 Alpine PT path reconstructed for the northern Dora-Maira Massif according to the results obtained from

metagabbro and metapelite samples. The PT path of Borghi *et al.*, (1996) for Dora-Maira and that of Le Bayon *et al.* (2006) for Gran Paradiso are reported for comparison.

Table 1 Sketch of the mineral assemblages related to the different deformation events and metamorphic conditions.

Table 2 Selected microprobe analyses for metapelite SU5 from the northern border of the Dora-Maira Massif.

Table 3 XRF composition (A) and chemical composition used for pseudosection modelling of Fig. 9 (B).

Figure 1

Click here to download high resolution image

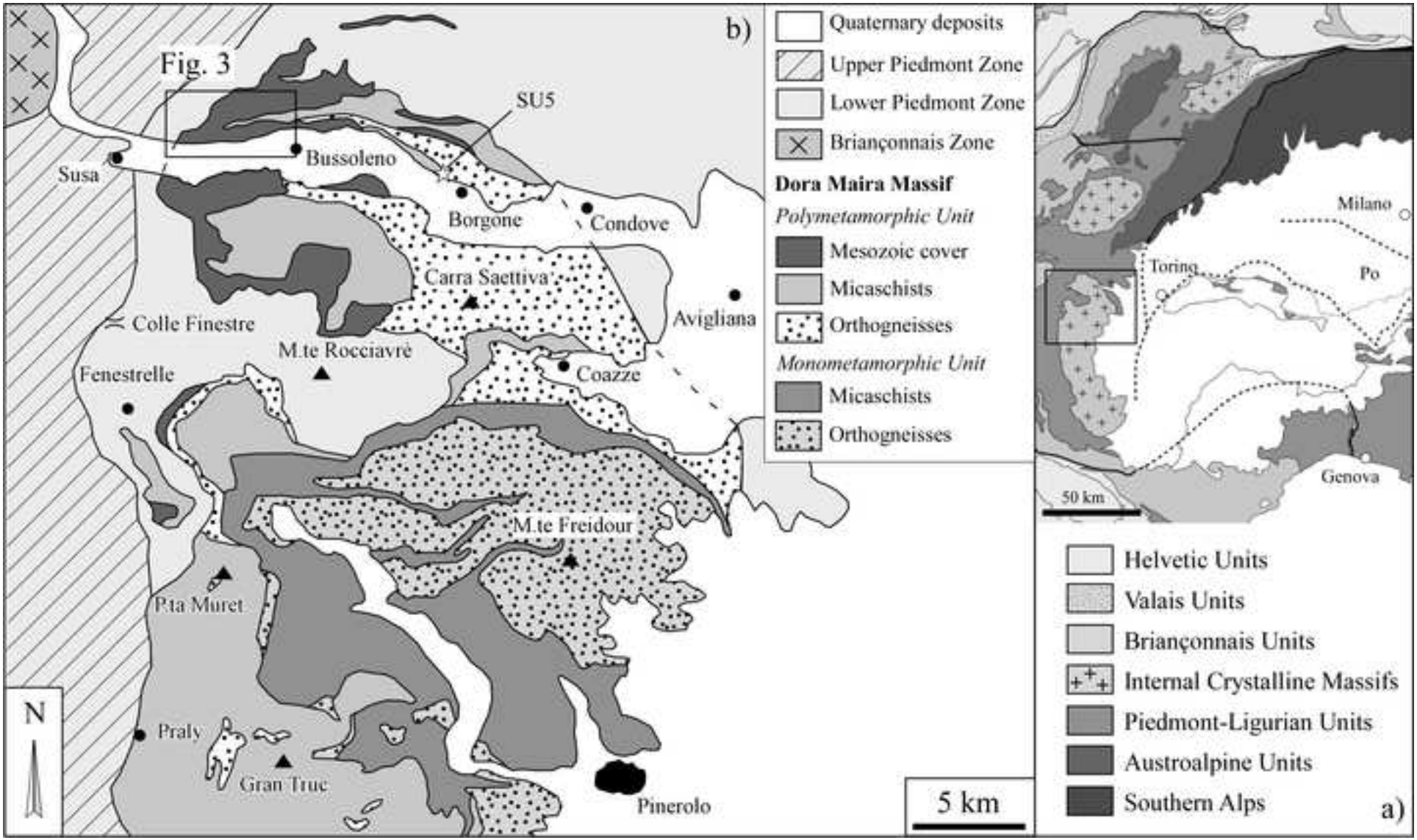

Figure 2

Click here to download high resolution image

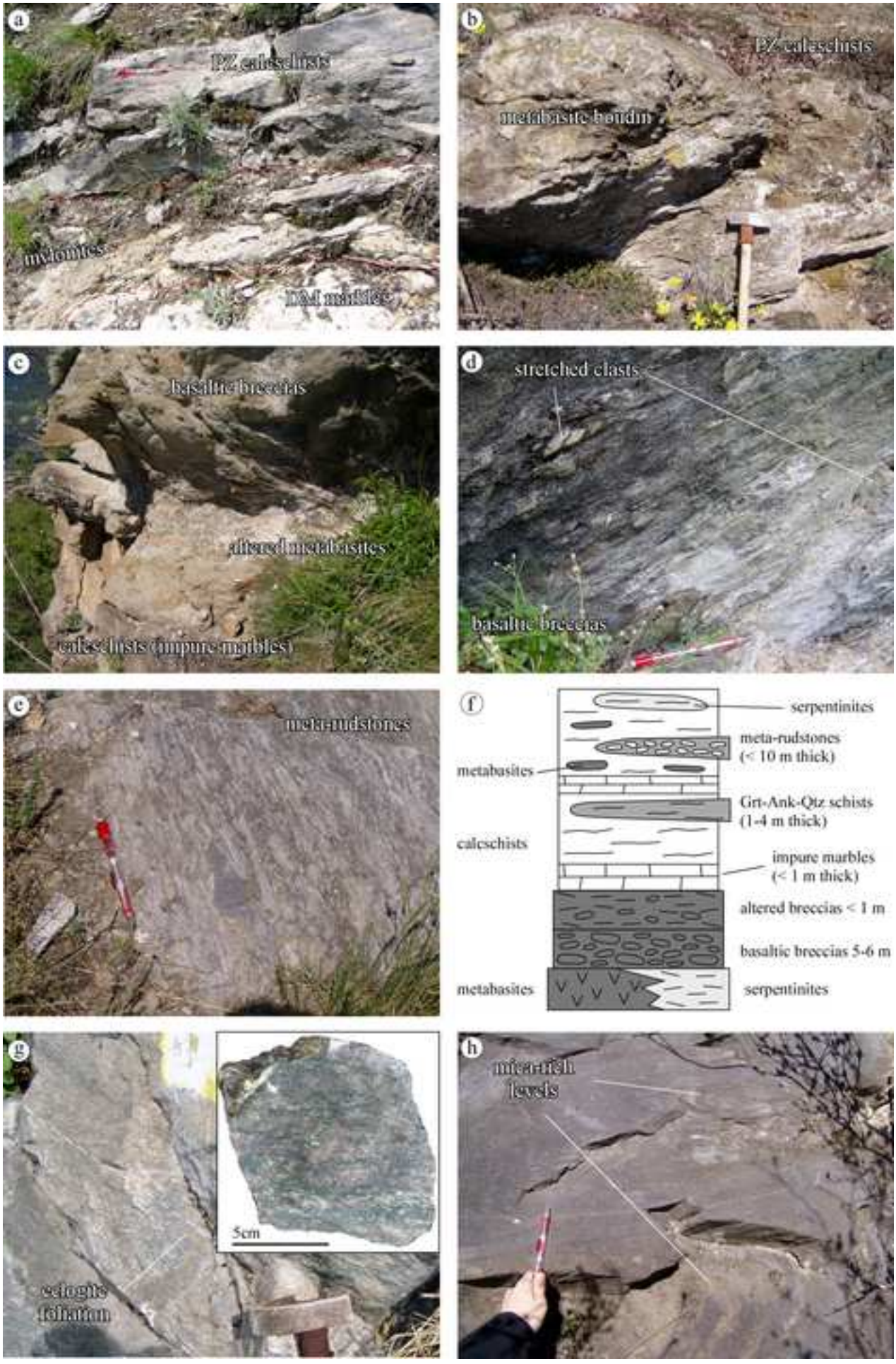

Figure 3

Click here to download high resolution image

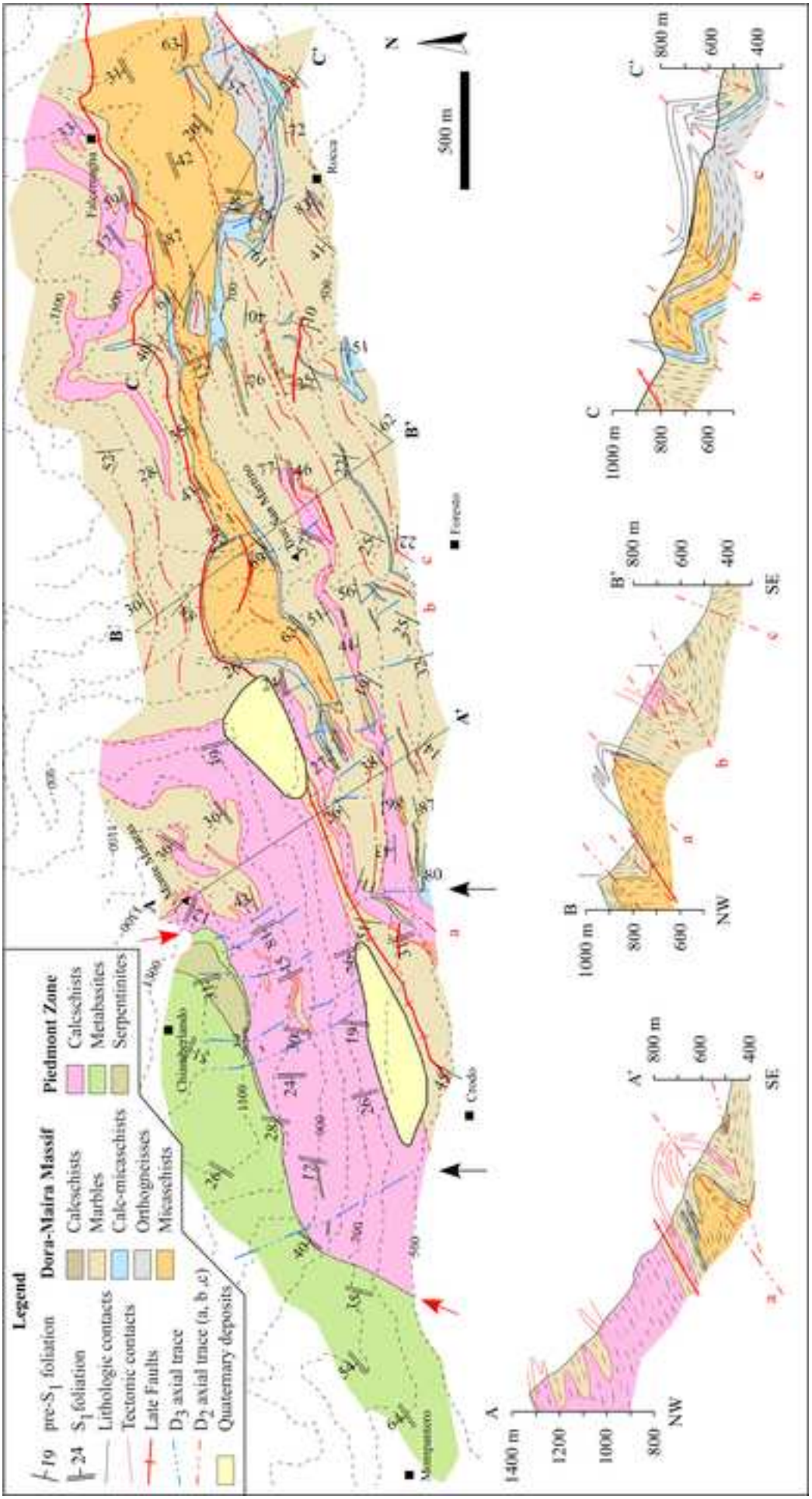

Figure 4

Click here to download high resolution image

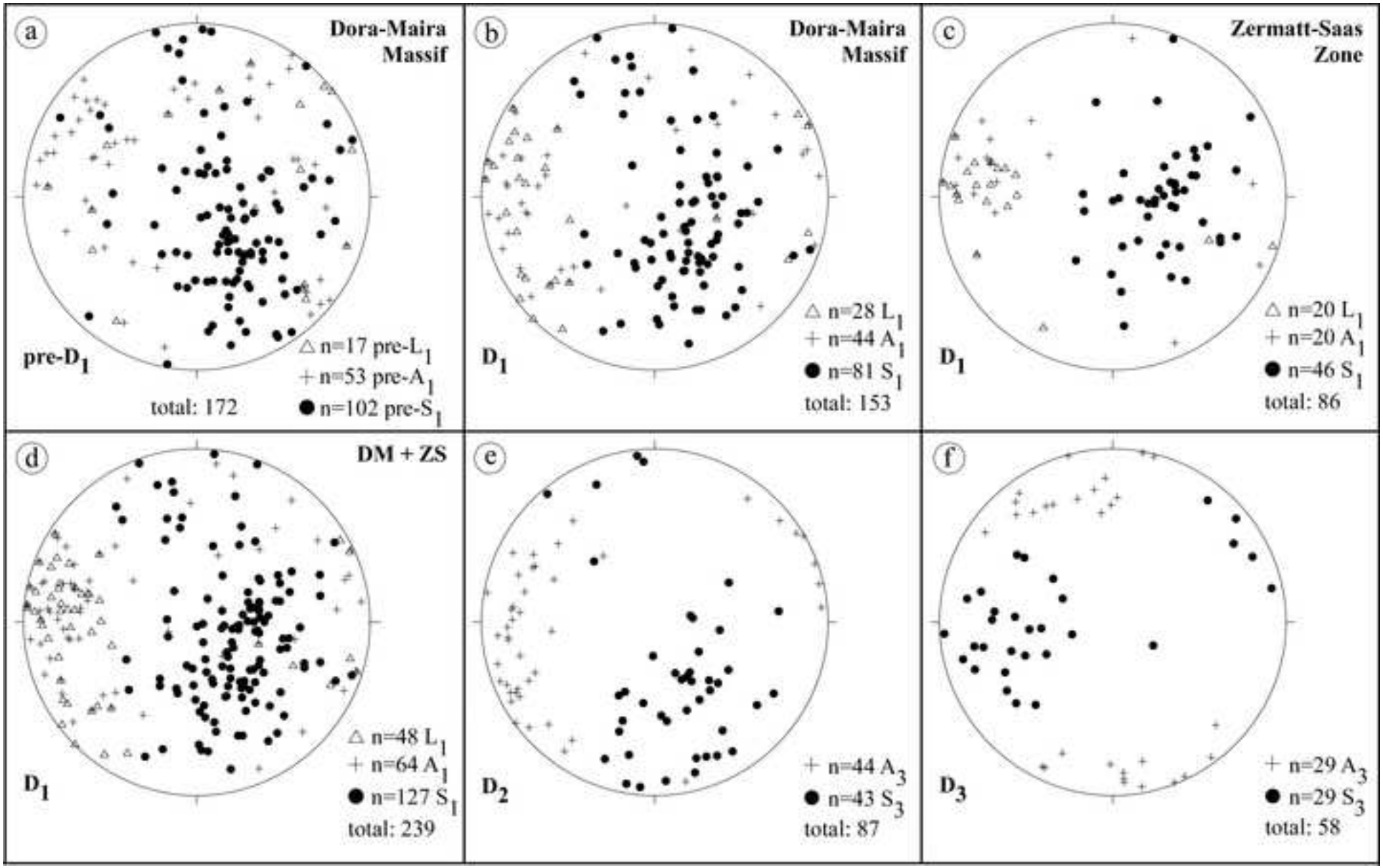

Figure 5

Click here to download high resolution image

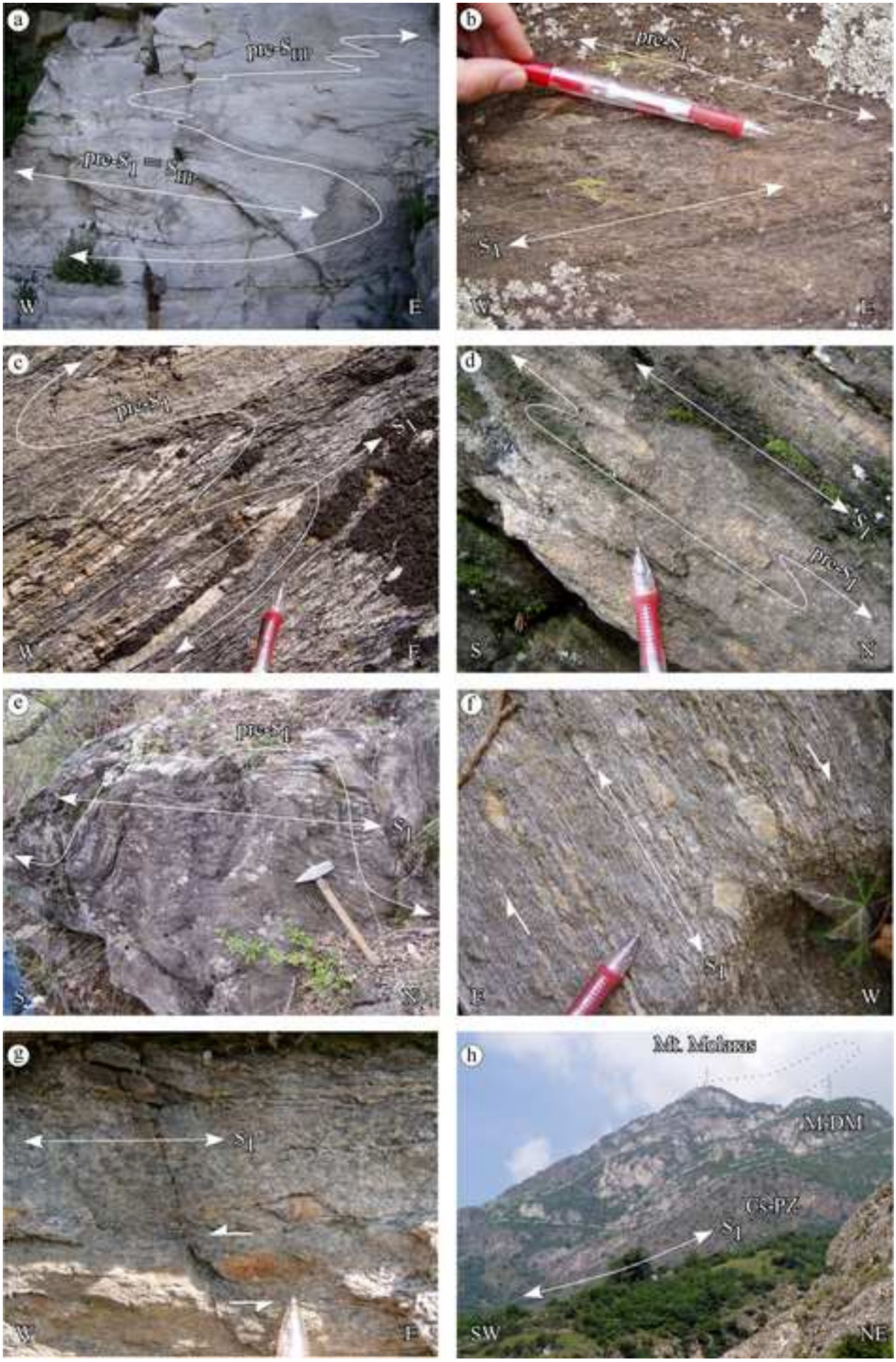

Figure 6

Click here to download high resolution image

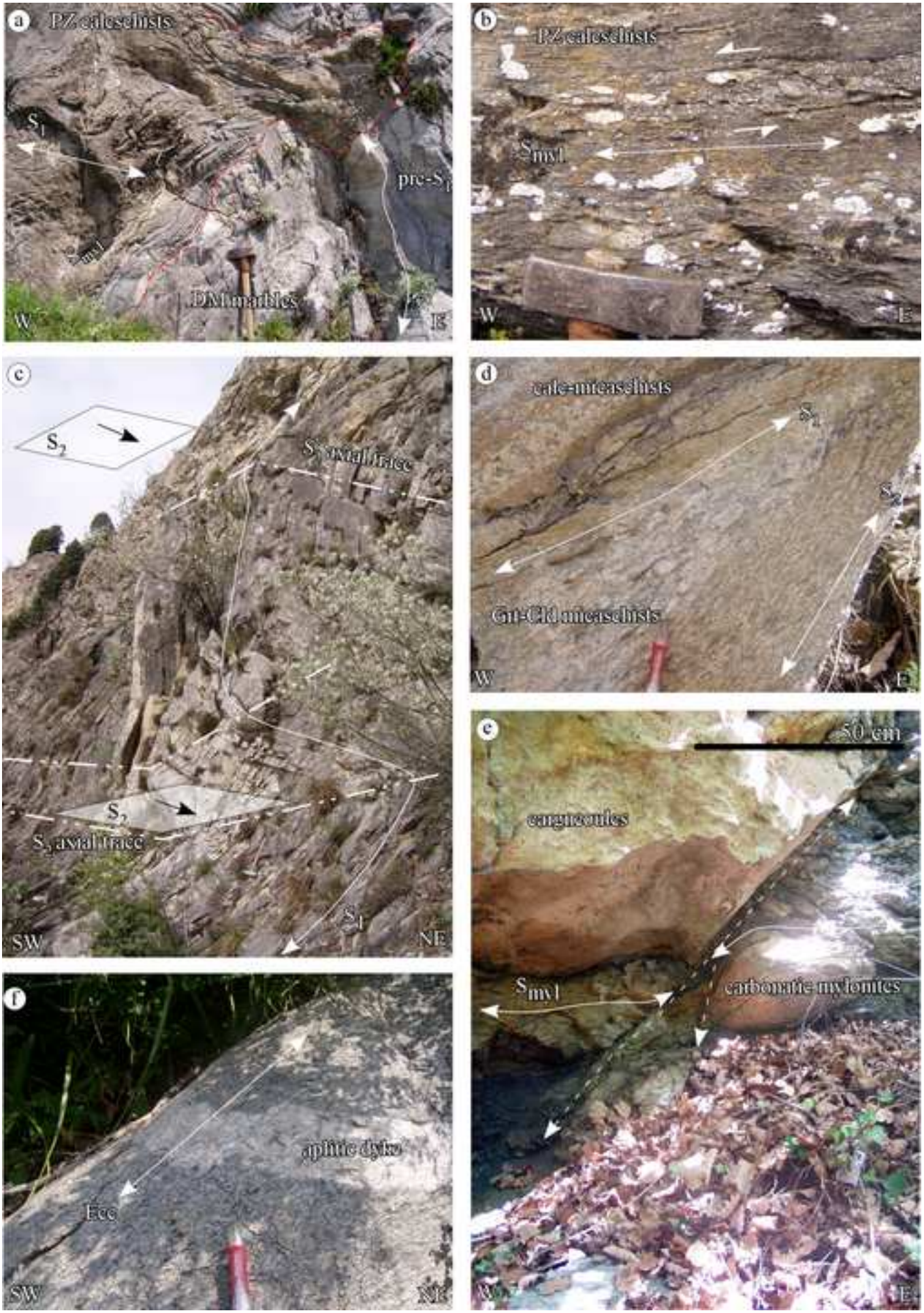

Figure 7

Click here to download high resolution image

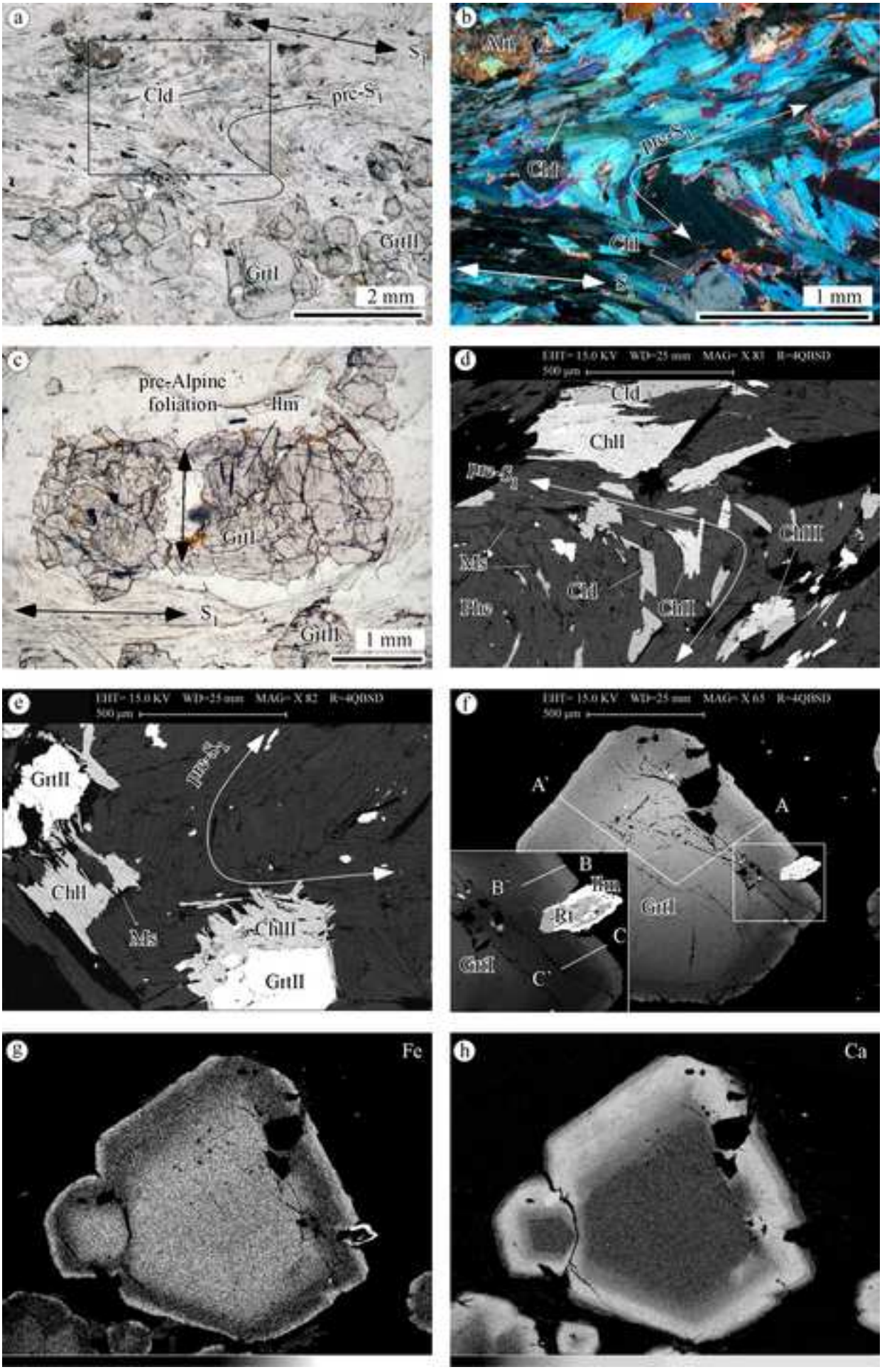

Figure 8

Click here to download high resolution image

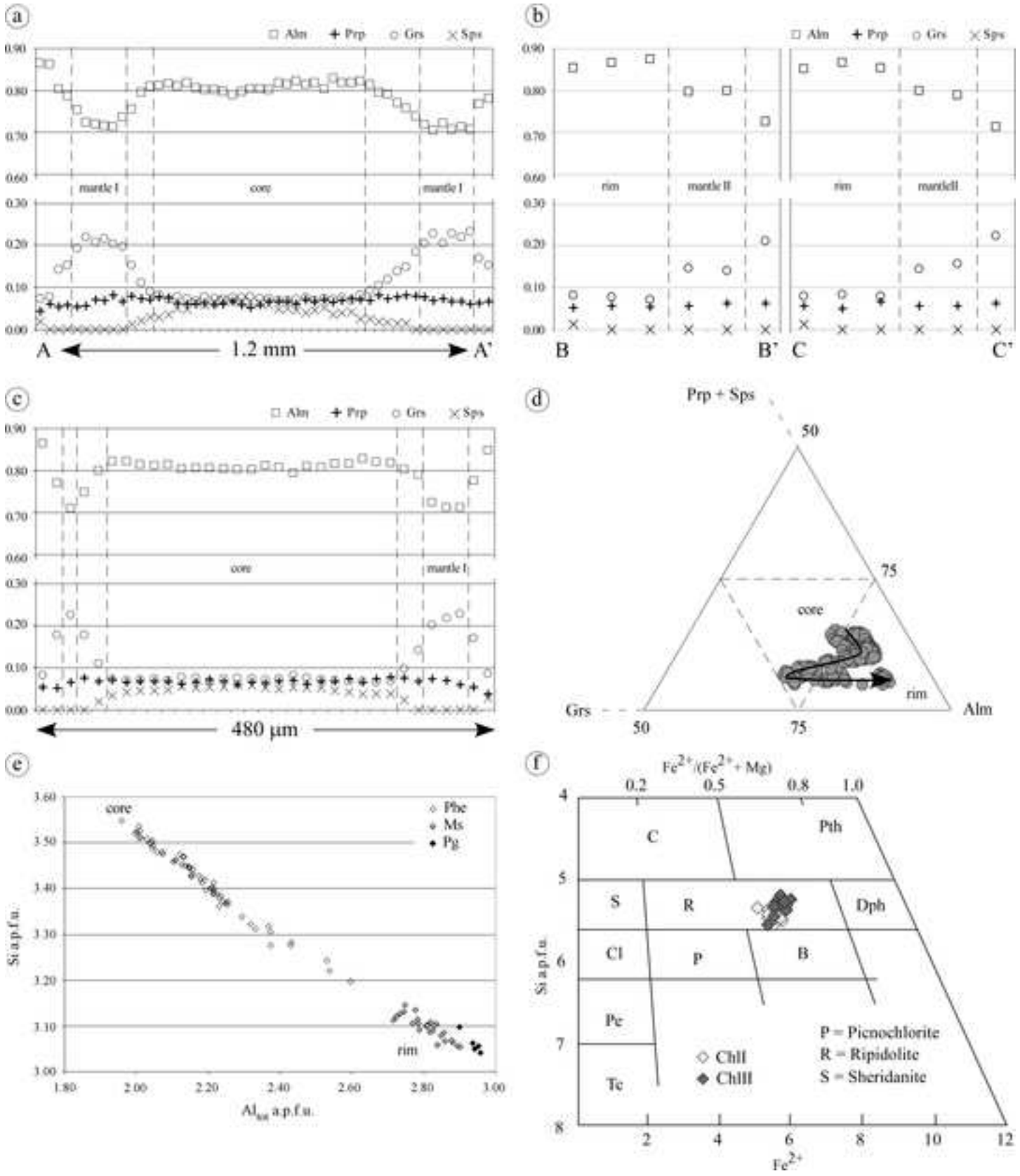

Figure 9

Click here to download high resolution image

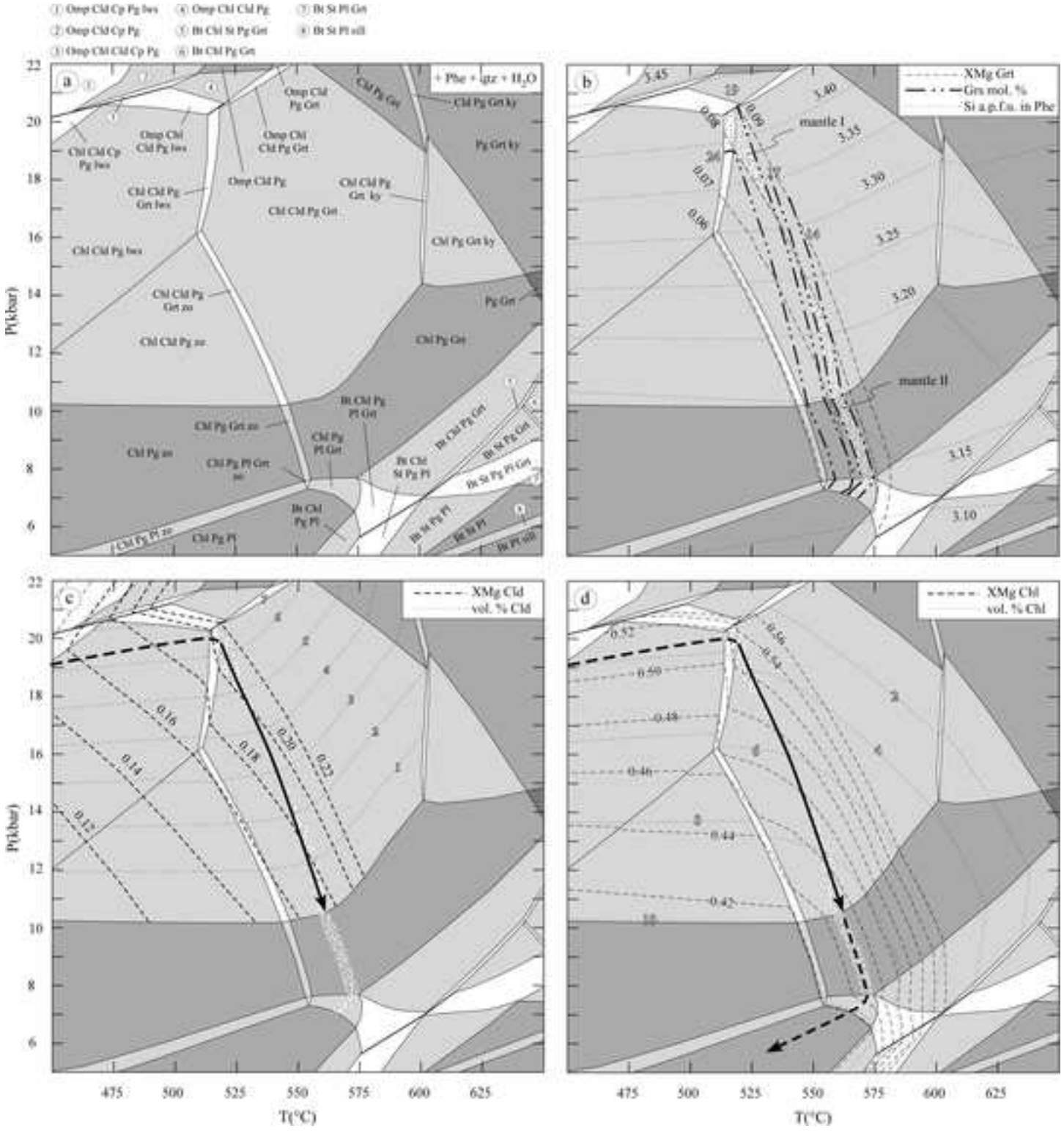

Figure 10

Click here to download high resolution image

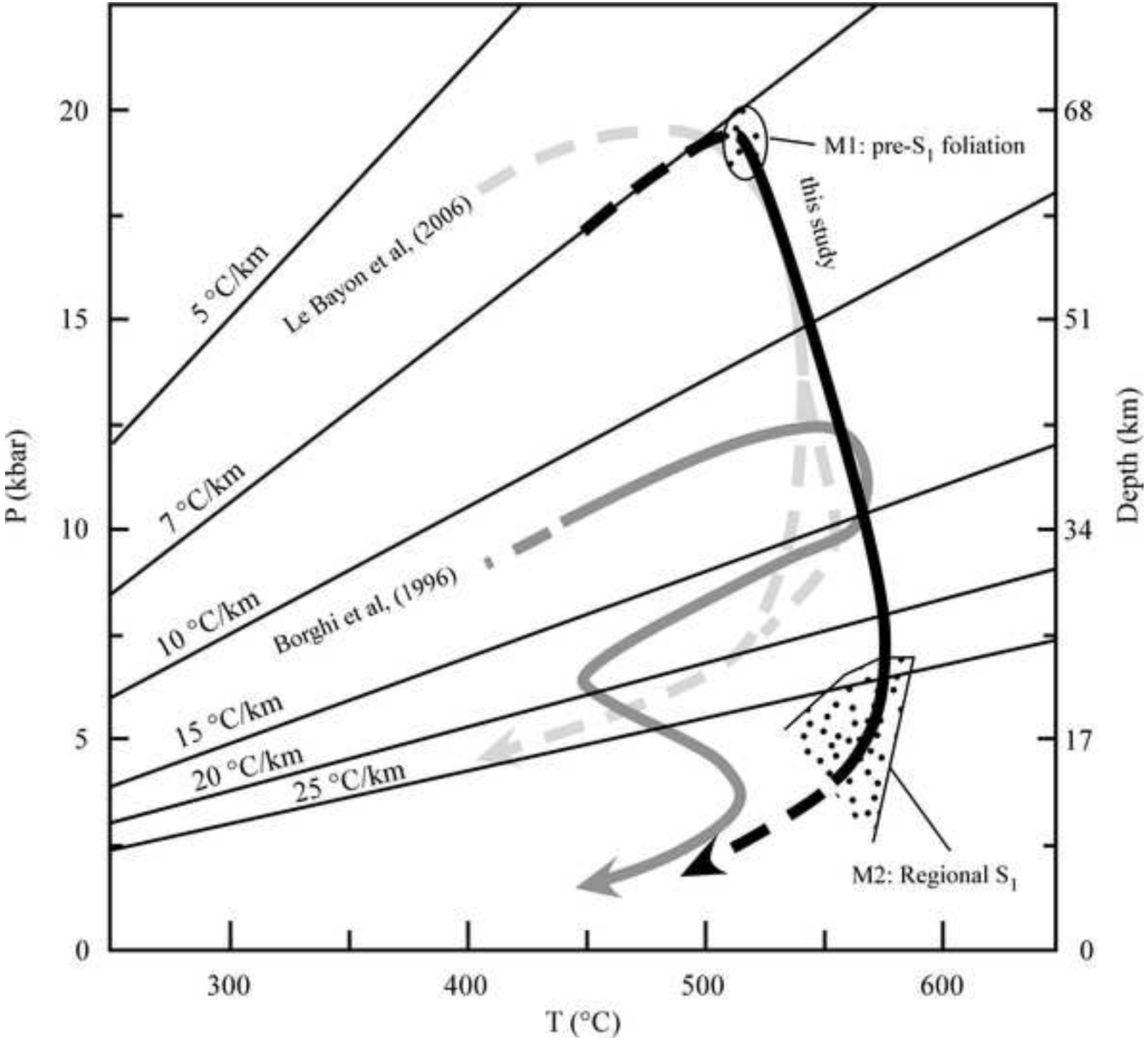

Table 1

Click here to download high resolution image

		Dora-Maira Massif		*Piedmont Zone*	
structural evolution	***metamorphic conditions***	micaschists	metabasites	calcschists	metabasites
pre-S_1	**eclogite facies**	Grt,Cld,Wm, Qtz, Rt	Omp, Grt, Ep, Wm, Cal, Spn	Grt, Wm, Qtz	Grt, Rt (relics)
S_1	**middel-P greenschist to epidote-albite amphibolite facies**	Wm, Qtz, Chl, Ab/Olig, Ilm, Bt(±)	-	Cal, Wm, Qtz, Chl, Spn	Chl, Ep, Ab Qtz, Spn, Cam(±)
S_2	**greenschist facies (?)**	Wm	-	-	-
S_3	**greenschist facies (?)**	-	-	-	-

Table 2

Click here to download high resolution image

	Grt*	Grt*	Grt*	Grt*	Wm*				Cld*		Chl*	
Analysis	grt24	grt45	grt55	grt53	wm43	wm119	wm12	wm37	cld56	cld14	chl4	chl48
Position	core	mantle I	mantle II	rim	core	rim						
					Phe	Phe	Ms	Pg			ChlI	ChlII
SiO_2	36.61	36.75	37.17	36.57	53.07	51.46	47.53	48.43	25.01	24.89	25.02	24.22
TiO_2	0.00	0.00	0.00	0.00	0.00	0.00	0.00	0.00	0.00	0.00	0.00	0.00
Cr_2O_3	0.00	0.00	0.00	0.00	0.00	0.00	0.00	0.00	0.00	0.00	0.00	0.00
Al_2O_3	20.00	21.04	21.14	20.49	25.60	29.73	36.14	39.70	40.17	40.82	21.81	20.74
FeOtot	35.88	31.95	35.60	38.60	3.09	2.98	1.15	0.00	25.83	25.10	31.08	31.53
MnO	3.04	0.00	0.00	0.00	0.00	0.00	0.00	0.00	0.00	0.00	0.00	0.00
MgO	1.45	1.74	1.41	1.41	3.21	2.41	0.61	0.00	2.09	2.40	10.99	9.94
NiO	0.00	0.00	0.00	0.00	0.00	0.00	0.00	0.00	0.00	0.00	0.00	0.00
CaO	2.63	8.06	5.07	2.69	0.00	0.00	0.00	0.00	0.00	0.00	0.00	0.00
Na_2O	0.00	0.00	0.00	0.00	0.00	0.35	1.19	6.76	0.00	0.00	0.00	0.00
K_2O	0.00	0.00	0.00	0.00	10.92	9.70	9.92	1.03	0.00	0.00	0.00	0.00
Sum	99.61	99.54	100.39	99.76	95.89	96.63	96.54	95.92	93.10	93.21	88.90	86.43
Si	3.005	2.966	2.993	2.993	3.523	3.368	3.106	3.055	2.059	2.038	5.348	5.370
Ti	0.000	0.000	0.000	0.000	0.000	0.000	0.000	0.000	0.000	0.000	0.000	0.000
Cr	0.000	0.000	0.000	0.000	0.000	0.000	0.000	0.000	0.000	0.000	0.000	0.000
Al	1.935	2.002	2.007	1.977	2.002	2.293	2.785	2.953	3.899	3.941	5.497	5.421
Fe^{3+}	0.000	0.000	0.000	0.000	0.000	0.000	0.000	0.000	0.000	0.000	0.000	0.000
Fe^{2+}	2.463	2.158	2.397	2.642	0.171	0.163	0.063	0.000	1.779	1.719	5.557	5.846
Mn	0.211	0.000	0.000	0.000	0.000	0.000	0.000	0.000	0.000	0.000	0.000	0.000
Mg	0.181	0.209	0.169	0.172	0.317	0.235	0.060	0.000	0.256	0.293	3.502	3.283
Ni	0.000	0.000	0.000	0.000	0.000	0.000	0.000	0.000	0.000	0.000	0.000	0.000
Ca	0.231	0.697	0.438	0.236	0.000	0.000	0.000	0.000	0.000	0.000	0.000	0.000
Na	0.000	0.000	0.000	0.000	0.000	0.044	0.150	0.840	0.000	0.000	0.000	0.000
K	0.000	0.000	0.000	0.000	0.924	0.809	0.828	0.083	0.000	0.000	0.000	0.000
Sum	8.026	8.032	8.004	8.020	6.937	6.912	6.992	6.931	7.993	7.991	19.904	19.920

*assuming all ferrous iron

Table 3

Click here to download high resolution image

wt. %	A	B
	XRF	*- Grt core*
SiO_2	69.38	70.06
Al_2O_3	18.46	18.41
FeO	4.69	4.06
CaO	0.14	0.08
MgO	1.64	1.64
Na_2O	1.13	1.15
K_2O	3.58	3.65
MnO	0.04	-